

**Student Name:** Mark Xu

**Date:** August 8, 2014

**Project Title:** Exploring cellular pathology after rotator cuff tears: implications of a shift towards fast fibers and increase in angiogenesis for repair and rehabilitation

**Primary Supervisor Name:** Dr Jeff Leiter, Dr Peter MacDonald

**Department:** Department of Orthopedic Surgery, Department of Anatomy & Cell Science

**SUMMARY:**

Supraspinatus tears are common in orthopaedic clinical practice but there is a gap in the literature regarding the natural history of rotator cuff pathology which compromises our ability to predict the potential recovery success following surgical repair. Previous studies have examined fatty infiltration, atrophy, MRI occupancy ratio, tangent sign, and Goutallier scores as predictors for the functional recovery of muscle, but there are scarce data investigating the cellular and molecular pathology of rotator cuff tears. This study investigated the fiber-type composition and myosin heavy chain protein (MyHC) (I/slow, II/fast: IIa, IIx, IIb) and vascular endothelial growth factor (VEGF) of pathological supraspinatus via immunohistochemistry and western blot. Corresponding clinical and MRI data were used to identify factors that may influence recovery. Biopsies (n=27) from torn supraspinatus and control muscle (deltoid) were retrieved during arthroscopic rotator cuff repair surgery. Torn supraspinatus demonstrated  $44 \pm 1\%$  slow fibers vs.  $57 \pm 1\%$  in control muscle ( $p < 0.01$ ), while the proportion of intermediate or transitional fibers (mixed positive and negative staining) did not differ ( $3.4 \pm 0.4\%$  in supraspinatus, vs.  $2.8 \pm 0.3\%$  in control). Differences in sex, smoking history, time from injury to surgery, and MRI data did not correlate with fiber type or myosin. VEGF was higher in pathological muscle ( $p < 0.05$ ). A shift towards fast fibers and greater VEGF suggests supraspinatus injury, consistent with disuse and/or denervation. These results together with muscle innervation status can provide insight into the overall health of the rotator cuff and allow us to better predict its ability to recover following injury.

**ACKNOWLEDGEMENTS:**

I gratefully acknowledge the support by one or more of the following sponsors:

H.T. Thorlakson Foundation  
Dean, Faculty of Medicine  
Manitoba Health Research Council  
Manitoba Institute of Child Health  
Kidney Foundation of Manitoba  
Leukemia and Lymphoma Society of Canada

CancerCare Manitoba  
Manitoba Medical Service Foundation  
Associate Dean (Research), Faculty of  
Medicine  
Heart and Stroke Foundation  
Health Sciences Centre Research  
Foundation

Other: Pan Am Clinic Foundation  
Alexander Gibson Fund  
Canadian Orthopaedic Research Legacy Grant (J Leiter, P MacDonald & J Anderson)  
MMCF - Reverend Thomas Alfred Payne Scholarship

## INTRODUCTION

Management of rotator cuff tears is complex. The clinical presentation can vary from severe disability to virtually no pain at all, and the decision to pursue surgical repair requires the consideration of many factors. Indications for surgery have been suggested in the literature<sup>1,2</sup>, but according to a survey conducted by the American Academy of Orthopaedic Surgeons, there appears to be a lack of agreement regarding these indications and variation in surgical decision-making<sup>3</sup>. More than 75,000 rotator cuff repair surgeries are performed annually in the United States<sup>4</sup> with the majority producing satisfactory outcomes, but studies have reported high failure rates ranging from 20% to 39% overall, and 41% to 94% at 2 years post-op in tears greater than 2cm<sup>5</sup>.

Although rotator cuff surgery restores structure, deficits in muscle strength and function can be seen. Presently, the natural history of rotator cuff pathology remains unclear<sup>6</sup> and few studies have examined biopsy samples taken during arthroscopic rotator cuff repair surgery. Because the histochemical and biochemical properties of muscle correlate with its function<sup>7</sup>, this study investigated the fiber-type composition, myosin heavy chain protein (I/slow, II/fast: IIa, IIx, IIb) and the signal for angiogenesis (VEGF: vascular endothelial growth factor) of pathological supraspinatus. Exploring the cellular and molecular characteristics of pathological rotator cuff muscle can help explain the variability in tissue quality and repair success rates, and provide insight into decisions for surgery and rehabilitation.

## Anatomy of the Shoulder Joint

The anatomic structure of the shoulder allows for extensive mobility greater than any other joint in the body. Three bones articulate at the shoulder: the clavicle, scapula, and proximal humerus. Together, they form two joints: the glenohumeral and acromioclavicular joint. Of relevance to this study, the glenohumeral joint is a multiaxial synovial ball and socket joint formed by the articulation between the humeral head and the glenoid fossa of the scapula. The shallow depth of the glenoid fossa and limited contact between this fossa and the humeral head contribute to the increased mobility of this joint, but at the same time enhance its susceptibility to injury and instability<sup>8</sup>. Stabilization and control of the glenohumeral joint is accomplished through the superior, middle and inferior glenohumeral ligaments, as well as the four deep rotator cuff muscles: the supraspinatus, infraspinatus, teres minor and subscapularis muscle. All rotator cuff muscles originate at different locations on the scapula and insert around the humeral head, collectively forming a tight cuff.

The supraspinatus originates from the supraspinous fossa of the scapula, located superior to the scapular spine, and passes laterally under the acromion, inserting most superiorly on the greater tuberosity. It contributes to the first 10 to 15 degrees of arm abduction, after which the lateral deltoid becomes the main propagator of abduction at around 30 degrees. As the deltoid abducts the arm, the rotator cuff muscles collectively stabilize the glenohumeral joint by preventing superior subluxation of the humeral head against the acromion. External rotation of the arm is accomplished by the infraspinatus and teres minor, which also insert on the greater tuberosity but on the posterior and inferior facet, respectively. The largest rotator cuff muscle, the subscapularis, internally rotates the arm, and originates on the anterior scapula to attach anteriorly onto the lesser tuberosity.

The suprascapular nerve typically arises from the C5 and C6 nerve roots of the brachial plexus, and provides innervation to the supraspinatus and infraspinatus. It courses under the superior transverse scapular ligament to innervate the supraspinatus, and then travels around the lateral border of the scapular spine and under the inferior transverse scapular ligament in the spinoglenoid notch to supply the infraspinatus<sup>9</sup>. The nerve is susceptible to compression and

injury at certain points along its pathway, most notably at the suprascapular notch and spinoglenoid region, leading to weakness in both supraspinatus and infraspinatus as well as infraspinatus alone, respectively. Typically, the nerve supplies two motor branches to the supraspinatus, one motor branch to the infraspinatus, and sends sensory fibers to the glenohumeral and acromioclavicular joint capsules<sup>9</sup>.

### **Mechanism of Injury**

The supraspinatus is the most commonly injured rotator cuff muscle<sup>10</sup>. It can be injured acutely from trauma, resulting in a full or partial thickness tear. However, in the general population, tears of a chronic nature are more common. These chronic tears are typically caused by both extrinsic and intrinsic factors. Extrinsic factors result from impingement of the muscle or tendon by surrounding bone or soft tissue<sup>11</sup>. During abduction of the arm particularly beyond 90 degrees, the bursal side of the supraspinatus is susceptible to direct mechanical compression in the subacromial space between the greater tubercle and acromion, and can compress against the coracoacromial ligament, anterior third of the acromion, and even the long head of the biceps<sup>12</sup>. Variations in acromial shape such as a hooked shape can also predispose to increasing friction and tear rates of the supraspinatus<sup>13</sup>. Intrinsic factors focus on the degenerative changes within the muscle and tendon that lead to rotator cuff tears. The mechanisms for these degenerative changes are an area of ongoing research, with studies investigating aspects such as aging, vascularization, innervation, and tensile stretch. Studies have indicated that aging is a major cause of degeneration and results in structural and functional changes, including collagen abnormalities and weakening of the tendon, which can be responsible for the tears when exposed to trauma<sup>14</sup>. Failure of appropriate response to stretch and load on the muscle and tendon can lead to oxygen free radicals and apoptotic signals, which weaken the collagen structure and cause degeneration ultimately leading to tear<sup>15</sup>. As well, some studies suggest there is an area of hypovascularity known as the "critical zone" on the supraspinatus tendon particularly susceptible to degeneration. Together, these factors affect the ability of the supraspinatus to function and heal.

### **Histopathology of Rotator cuff tears**

Fatty infiltration, muscle fibrosis and muscle atrophy tend to correspond with poor tissue quality and poor rotator cuff healing following chronic tears<sup>16</sup>. In chronic rotator cuff tears, the tear can lead to mechanical unloading and retraction of the muscle belly and tendon, resulting in an increased pennation angle which is the angle between the muscle fibers and long axis of the tendon. Consequently, interstitial fat and fibrous tissue can accumulate in the enlarged spaces between the newly reoriented muscle fibers<sup>17</sup>. The cause of this fatty infiltration and fibrosis is unclear. At a molecular level, studies have suggested that one of the key regulators of this process is peroxisome proliferator-activated receptor gamma (PPAR-gamma), which controls gene expression for fat cell differentiation<sup>18</sup>. Denervation of the suprascapular nerve may also contribute to this change<sup>19</sup>. Studies have suggested that severe fatty infiltration appears at an average of 5 years following onset of pain<sup>20</sup>. Muscle fibrosis is detrimental to muscle quality as myofibers are progressively replaced by extracellular matrix proteins, as seen in some muscular dystrophies.

Muscle atrophy is also observed with chronic tears. Normally, muscle responds to mechanical loading and upregulates protein synthesis for growth and maintenance. When the muscle is torn, this loading diminishes and atrophy-related proteins such as nuclear factor kappa B and forkhead transcription factor take effect<sup>21</sup>. A study demonstrated decreased muscle mass and cross-sectional area following tenotomy in an animal model, as well as after denervation<sup>22</sup>.

## **Muscle Fiber typing**

The fiber-type composition of muscle dictates the muscle's function and performance. Muscle fibers are made up of sarcomeres, which feature the myofibrillar proteins myosin and actin interacting with each other to produce muscular contraction. The myosin protein is also known as the thick filament and contains 2 heavy and 4 light polypeptide chains. The myosin heavy chain (MyHC) contains the myosin head which comes into contact with actin and produces muscular contraction in a process known as cross-bridge cycling. Here, the myosin attaches to actin, pulls it in the direction of muscular contraction, releases and reattaches again.

Additionally, the heavy chain also contains ATPase, an enzyme that hydrolyzes ATP to provide energy for the contraction. The rate that ATPase hydrolyzes ATP largely determines how fast that muscle can contract. Human skeletal muscle features several isoforms of this myosin heavy chain, each with its own metabolic profile: MyHC type I, IIa, IIx, and IIb. Type I isoforms contract slowly and are more resistant to fatigue, while type IIb isoforms allow for very fast contraction and fatigue quickly. Type IIa and IIx are considered transitional isoforms that contract at speeds in between type I and IIb isoforms. Because muscle responds to demand in adaptation, a fiber can contain more than one type of myosin isoform.

Overall, individual fibers can be typed as either slow-twitch or fast twitch. Slow-twitch (type I) fibers are abundant in mitochondria and their energy is largely supplied by oxidative metabolism. On the other hand, fast-twitch fibers (type II) rely more on glycolytic metabolism for energy and are more prone to fatigue, and can also be further broken down into type IIa, IIx, and IIb. Fiber-type composition features a high degree of plasticity.

A shift in fiber-type composition can provide insight into the overall health and function of human skeletal muscles. Several studies have demonstrated that exercise and training can produce a shift in muscle fiber type composition towards slow-twitch type I fibers<sup>23</sup>. Conversely, mechanical unloading of muscle results in a decrease of slow-twitch muscles and increased proportion of fast-twitch muscles, possibly related to a disuse phenomenon or denervation. In fact, studies have demonstrated that in long-term muscle paralysis seen in spinal cord injury individuals, there likewise exists a shift towards fast fibers and decreased amounts of slow fibers even though muscle cross-section area and peak muscle force remained similar to control groups<sup>24</sup>. Uninjured muscle and regular use tend to maintain fiber type composition and morphology, fiber size and MyHC expression even in ageing skeletal muscle<sup>25</sup>. Changes in fiber type composition can contribute to the disabilities experienced by individuals who suffer from muscle denervation or immobilization<sup>26</sup> and examination of a shift in fiber type composition can help describe the overall muscle condition, even before muscle atrophy manifests<sup>24</sup>.

## **Vascularization**

Because myonuclei are post-mitotic, the mature muscle cell cannot divide and regenerate by itself following injury. Instead, satellite cells are the stem cells of the muscle and initiate proliferation and differentiation into myoblasts which fuse to form nascent fibers<sup>27</sup>. Moreover, repair of muscle tears require sufficient oxygen and nutrients, which are supplied by blood vessels. Revascularization during the process of muscle regeneration is critical and highly active.

Angiogenesis refers to the growth of blood vessels from existing vessels, and can be described by two processes: intussusception and sprouting<sup>28</sup>. Intussusception angiogenesis, also known as splitting angiogenesis, occurs when a transluminal pillar forms in the injured vessel segment and splits it into two new vessels<sup>29</sup>. Stimuli for intussusception results predominately from increased shear stress and blood flow<sup>30</sup>. On the other hand, sprouting angiogenesis occurs when new capillaries extend from the basement membrane of an existing capillary and grow towards the area of injury<sup>31,32</sup>.

Notably, the key regulator for angiogenesis is vascular endothelial growth factor (VEGF). VEGF has direct mitogenic effects on endothelium by acting on two tyrosine kinase receptors on endothelial cells: fms-like tyrosine kinase (flt-1) and kinase insert domain-containing receptor/fetal liver kinase-1 (KDR/Flk-1). The VEGF activation of endothelial cell proliferation involves several pathways including the mitogen-activated protein kinase (MAPK) pathway, the extra-cellular-signal regulated-kinase-1/2 (ERK1/2) pathway, as well as activation of factors such as stress-activated protein kinase 2 (SAPK2) and anti-apoptotic kinase Bcl2 and A1<sup>33</sup>. In injured muscle, previous studies have shown that VEGF protein significantly increases at locations of new vessel formation during muscle repair<sup>34</sup>. Studies have indicated that VEGF is the main regulator for angiogenesis during muscle injury<sup>33</sup>. Not surprisingly, hypoxia in the muscle seems to be the primary activator of VEGF<sup>35</sup>.

Several studies have investigated the role of VEGF particularly during embryonic development. VEGF-knock-out is lethal<sup>33</sup>, and embryos that are heterozygous for VEGF exhibit abnormalities in growth and development. As well, inactivation of VEGF seems to fully suppress angiogenesis in certain areas such as hypertrophic cartilage<sup>33</sup>.

### **Hypothesis**

This study proposes that: (1) supraspinatus muscle from individuals undergoing surgery for a torn supraspinatus tendon will exhibit a change in fiber-type composition and VEGF signal for vascularization versus control muscle. (2) Age, sex, smoking history and prolonged time from injury or pain onset to surgery can account for the difference in fiber type composition. (3) MRI tangent sign, occupancy ratio, and Goutallier score can account for the difference in fiber-type composition. (4) There is a correlation between fiber-type composition and vascularization signal.

### **Clinical significance**

Previous studies have examined VEGF with respect to the different muscle fiber types. Exercise-induced increase in VEGF expression is elevated in type IIb fibers more than the other muscle fiber types<sup>36</sup>. Type II fibers primarily rely on glycolytic energy metabolism and are more susceptible to hypoxia than the other type I which uses oxidative energy metabolism more readily<sup>36</sup>. Thus, knowledge of the amounts of expressed angiogenesis signal and transformation of fiber-type composition from control muscle can describe tissue quality and its susceptibility to hypoxia, providing insight into whether the muscle is prone to tearing and its ability to regenerate itself following injury. Knowledge of the fiber type composition is also useful to develop more personalized rehabilitative protocols for individuals with rotator cuff tears, taking note of the amount of slow vs. fast type fibers in injured muscle.

## **MATERIALS AND METHODS**

This protocol received approval from the University of Manitoba (UM) Biomedical Research Ethics Board and the WRHA Research Access Committee for collection of muscle biopsy samples from patients undergoing arthroscopic rotator cuff repair surgery. All clinical work was performed at Pan Am Clinic, while biological-science activities took place in the department of Biological Sciences at the University of Manitoba.

Potential study participants were screened from the surgical waitlist of participating surgeons with the following inclusion criteria: aged 35-70 years, diagnosed with a rotator cuff tear of supraspinatus, failed conservative management, and satisfying all indications for rotator-cuff surgery<sup>37</sup>. Informed consent forms were completed prior to study participation.

### **Tissue Collection**

Muscle biopsies were obtained from the torn supraspinatus and unaffected ipsilateral deltoid via arthroscopic basket punch (4x4x4 mm<sup>3</sup>) during rotator cuff repair surgery at Pan Am Clinic. Biopsy samples were coded as “A” or “B” as a blind to minimize bias. In this study, the deltoid serves as a suitable control muscle according to previous studies<sup>38,39</sup>. Each biopsy was divided for histological study on frozen sections or protein expression analysis.

### **Cryostat sectioning**

In the operating room, biopsy portions dedicated for histological study were placed directly into 10mL 4% paraformaldehyde (PFA) and transported to the lab for processing. Samples were sectioned (International Cryostat Model CTI) at a thickness of 7µm onto silanated slides.

### **Immunohistochemistry (IHC)**

Fiber-type composition was assessed by identifying type I fibers using a monoclonal antibody to slow myosin (Stanford University School of Medicine, A4.951, diluted 1:50). IHC protocol was followed according to our previous studies<sup>40</sup>.

### **Microscopy Imaging and IHC Analysis**

Slides were imaged with an Olympus BH2 microscope at 10X magnification. Stained fibers were easily identifiable at this magnification; the entire section was imaged and all fibers counted to minimize bias. Positively stained fibers were counted as type I, and unstained fibers as non-type I. Fibers with intermediate staining were further classified as dark/medium stained, dark/non-stained, and medium/non-stained, and the total of these fibers served as an overall intermediate-fiber count representing fibers in transition between slow and fast fiber types. The type-I positive, negative and intermediate raw counts were recorded as a proportion of total fibers for each muscle sample.

### **Western blot (WB) & quenching**

Proteins were extracted from a portion of the biopsy sample, placed in RNA-later in the operating room, and run in 4% gels for immunoblotting according to standard protocols<sup>40,41</sup> to provide further assessment of fiber-type composition in pathological supraspinatus and control muscle. The VEGF vascularization signal was also quantified (9% gels). Membranes were incubated with mouse anti-IIb-MyHC (1:500) and visualized with secondary antibody (bovine anti-mouse-HRP. 1:5000) and the luminol detection system (Santa Cruz). Bands were imaged using a VersaDoc 4000MP system and the QuantityOne program V4.6.8 at 100s exposure. Following detection and imaging, membranes were quenched and re-probed with a pre-complexed antibody-cocktail solution of (1) mouse anti-IIx-MyHC (1:500, Stanford University School of Medicine, 6H1), goat anti-mouse HRP (1:5000), and mouse serum (1:250)<sup>41</sup>, (2) polyclonal rabbit anti-IIa-MyHC (1:400, 55069-1 AP, ProteinTech) and (3) mouse anti-I-MyHC (1:1000, Stanford, A4.951). ImageLab V3.0 was used to analyze band intensity. The concentrations of type-I MyHC isoform and specific isoforms for Type II fast-twitch fibers (IIa, IIx, and IIb), and VEGF, were expressed relative to a loading control protein, beta-actin, in each sample, and compared between pathological and control muscles. Goat anti-VEG-F (1:400, P-20: sc-1836, Santa Cruz Biotechnology Inc) and secondary antibody solution (bovine anti-goat-HRP (1:5000) were used following the same protocol.

### **Patient demographic data and MRI assessment**

Clinical assessment took place at Pan Am Clinic and demographic data was retrieved from the electronic medical record system at the facility. Compiled demographic data included: age, sex, body mass index (BMI), smoking history, timeline from pain/injury to MRI, and timeline from pain/injury to surgery.

Pre-operative MRI images were taken at the Pan Am Clinic Diagnostic Imaging Department with a 1.5T Siemens MAGNETOM scanner (Siemens, Erlangen, Germany), and assessed for tear size, tear thickness, and tendons involved. Furthermore, the tangent sign, occupancy ratio and Goutallier CT-scan classification adapted for MRI images were calculated. The tangent sign functions as a qualitative sign for supraspinatus muscle atrophy. The parasagittal T1-weighted scapular Y-view was obtained from the IMPAX imaging system for each study patient, and a line was traced from the superior border of the scapular spine to the superior margin of the coracoid<sup>42</sup>. The tangent sign is positive if the supraspinatus muscle does not cross above this line. To assess supraspinatus muscle atrophy, the occupancy ratio was calculated from the same scapular Y-view by dividing the cross-sectional area of the supraspinatus by that of the supraspinatus fossa. The ratios were compared to published standards<sup>42</sup>. Finally, the Goutallier classification adapted for MRI images grades fatty degeneration in supraspinatus in 5 stages<sup>43</sup>. Stage 0 suggests normal muscle and no fatty streaks. Stage 1 exhibits some fatty streaks. In Stage 2, there is significant fatty infiltration but still more muscle compared to fat. Stage 3 exhibits an equal amount of fat and muscle. In Stage 4, there is more fat than muscle present.

### **Data and Statistical analysis**

Paired t-tests were used to compare overall muscle fiber-type proportions and Western blot protein-quantification data for myosin isoforms to investigate differences between supraspinatus and deltoid control muscle. VEGF signal between supraspinatus and control was investigated by comparing the ratio of supraspinatus:control to a hypothesized mean of 1. Additionally, subjects were grouped according to various demographic and MRI data, and the differences in the proportion of type I fibers and MyHC and VEGF protein levels from Western blots were investigated with an analysis of variance (ANOVA) to determine the predictive value of biological studies with respect to demographic and MRI findings. JMP 10 was utilized to conduct statistical analysis, and the p-value was set at  $p < 0.05$  for significance.

## **RESULTS**

### **Demographics**

In total, 32 patients consented to the study, from which biopsies were retrieved from 27 patients (7 females, 20 males). Five participants were excluded following assessment in the OR as they did not meet the inclusion criteria for the study. For example, one individual did not have a supraspinatus tear via arthroscopy. Table 1 shows the overall study demographic data. Briefly, the average age of study participants was 57 years, with a range from 45 to 66. Smoking history was noted in 8 individuals. Average time from the start of injury or pain to surgery was 73 weeks. There was one subject with a very long timeline (520-week history of pain, prior to surgery). With this patient excluded, the average time from injury or pain to surgery was 55 weeks. However, that patient was included in all histological and MRI assessments.

### **MRI findings and measurements**

Table 2 shows the overall study MRI findings and MRI tangent sign, occupancy ratio, and Goutallier scores. Two subjects had a partial-thickness tear of the supraspinatus, while the others had full-thickness tears. Tangent sign was positive in three subjects, occupancy ratio averaged 0.79 (range: 0.31 to 1.15), and Goutallier score ranged from 0 to 3. In the three subjects with a positive tangent sign, the occupancy ratio was the lowest among this data set (0.35, 0.52, 0.57) and accounted for the two largest tears in our data set (AP 3.8, 4.6) according to MRI findings. Table 3 shows both demographic and MRI measurements for each patient.

### **Arthroscopy findings**

Arthroscopy confirmed the full thickness (n=25) and partial thickness supraspinatus tears (n=2) indicated by MRI. Rotator cuff repair was performed in all study participants.

### **Muscle fiber types and MyHC isoforms**

For each section, the entire biopsy sample was imaged and analyzed. In total, 31259 fibers were counted. IHC (Figure 1) showed a significant difference in the proportion of type-I fibers between pathological supraspinatus and control muscle ( $p < 0.001$ ). Torn supraspinatus muscle showed  $44 \pm 1\%$  slow fibers while control muscle showed  $57 \pm 1\%$ . There were  $53 \pm 1\%$  non-staining (fast) fibers in supraspinatus while control muscle showed  $40 \pm 1\%$  of non-stained fibers. Finally, intermediately stained fibers were  $3.4 \pm 0.4\%$  of fibers in pathological and  $2.8 \pm 0.3\%$  of fibers in control muscle (Figure 2).

Western blot for MyHC isoforms (type I, IIa, IIx, IIb) confirmed the heterogeneity of human pathological supraspinatus and control muscle and the shift toward faster fibers in the pathological muscle, but did not correlate significantly with the proportion of type-I fibers assessed by IHC (Figure 3).

For age, sex, smoking history, and time from pain or injury to surgery, there was a difference in fiber-type composition between pathological versus control muscle ( $p < 0.001$ ). However, fiber type within pathological supraspinatus could not be distinguished by studying the distribution of fiber types according to subsets of the aforementioned categories, and therefore did not correlate with these factors (Figure 4).

Interestingly, there was a difference in the proportion of type-I fibers between pathological and control muscles for individuals over and under age 60. For control muscle, the proportion of type-I fibers decreased with age ( $p < 0.05$ ). However, this was not the case for comparison of type-I fiber proportion by age-group in supraspinatus. This suggests the shift toward faster fiber-type composition is similar regardless of age (Figure 4a).

Similar to the demographic information, MRI tangent sign, occupancy ratio, and Goutallier score were different between pathological supraspinatus and control muscle ( $p < 0.001$ ) but did not correlate with MRI measures (Figure 5).

### **Vascularization**

VEGF (relative to actin) was greater ( $p < 0.05$ ,  $n=18$ ) in pathological supraspinatus ( $0.45 \pm 0.1$ ) compared to control ( $0.27 \pm 0.05$ ). (Figure 6). Additionally, correlation between type I slow fibers and VEGF angiogenesis signal showed a negative slope, but this was not significant ( $p > 0.05$ ) (Figure 7).

### **DISCUSSION**

Our results demonstrate an overall shift in fiber-type composition from 57% type I in control muscle to 44% in pathological supraspinatus muscle. Correspondingly, fast-twitch fiber proportions increased overall in pathological supraspinatus. The largest difference in the proportion of type I fibers in one subject of our data set was from 64% to 39%. This participant had a partial thickness tear in the absence of any other outstanding demographic or MRI features. On the other hand, only one participant had a higher proportion of type I fibers in pathological supraspinatus than control muscle, although the (non-significant) difference was almost negligible. This was a female subject with a full-thickness tear who also had no other exceptional demographic or MRI findings.

Our data are consistent with previous studies examining fiber-type changes following injury and immobilization<sup>44</sup>. In a similar study, Haggmark et al.<sup>44</sup> investigated fiber-type changes in biopsy samples taken during knee surgery from eight athletes, and found a strikingly similar decrease compared to control contralateral muscle in the percentage of type I fibers from an average of 54% to 43%, despite examining different muscles than in the present study. One individual from



the Haggmark et al. study showed a dramatically lower proportion of type I fibers from 81% on the control side to 58%. Interestingly, the study also examined the differences in fiber-type proportions between contralateral pairs of muscle in the injured versus non-injured leg and found a dramatic difference with 20% versus 69% type-I fibers, respectively. Immobilization and disuse of muscle produces profound changes in the muscle itself and also in its innervation<sup>44</sup>. The present study was consistent with Haggmark's paper.

Another study conducted by Scelsi<sup>45</sup>, examined fiber-type changes in paraplegics in the immediate months following a spinal cord injury. From one to six months, muscle atrophy occurred primarily in type II fibers without any deviation in the overall proportions of slow versus fast fibers. However, from eight months onwards, atrophy affected both types of fibers equally although type II fibers and fast MyHC isoforms increased and predominated<sup>45</sup>. This increased proportion of fast-twitch fibers helps explain the fatigability experienced by paraplegic individuals. Moreover, type II fibers are more susceptible to injury than type I fibers<sup>46</sup>. The degree to which fast fibers predominate following injury or aging<sup>47</sup> can provide insight into the overall muscle quality and function.

There are few studies describing the fiber-type composition of rotator cuff muscles. One study examined six cadaveric rotator cuff specimens and determined the fiber-type composition by IHC and WB of each rotator cuff muscle. Similar to our data, they reported heterogeneity in supraspinatus fiber-type proportions among specimens, and found supraspinatus had  $54 \pm 6\%$  slow myosin content, comparable to the  $57 \pm 1\%$  slow-fiber proportion in our control muscle.

Although our findings for fiber-type composition and MyHC isoforms were different in pathological supraspinatus versus control muscle with respect to sex, smoking history, time from symptom onset to surgery, MRI occupancy ratio, tangent sign, and Goutallier score, fiber type distribution could not be differentiated according to subsets of these categories. Thus, from our data, these factors do not seem to account for fiber-type changes seen in muscle, at least not in this cohort. These results are similar to those from a biopsy study on neck muscles conducted by Uhlig et al.<sup>48</sup> In that study, various neck muscles from individuals experiencing cervical dysfunction were biopsies and they also found a predominance of type II fibers in pathological muscle along with increased transitional fibers. They also compared the fiber-type composition of pathological neck muscles to factors such as age, sex, and type of condition but found no correlation with any of the three factors.

In our study, prolonged time from injury to surgery did not correspond to a decrease in slow-twitch fibers, but all pathological muscle displayed a consistently reduced proportion of slow-twitch fibers vs. control muscle from the same subject, suggesting the cellular changes within supraspinatus rotator cuff muscle happens acutely after a muscle tear.

Our WB quantification of MyHC isoforms did not significantly correlate with IHC fiber-type proportions. Although both methods aim to quantify the functional differences in fiber type in a muscle, they approach this in different ways. The WB protocol strictly quantifies the overall ratio of protein isoforms in a muscle (contributed by fibers corresponding to type I, IIa, IIx, and IIb), while IHC provides insight into overall fiber-type distribution and proportions in the muscle.

Not surprisingly, the VEGF-angiogenesis signal was greater in torn supraspinatus compared to control muscle. In a rabbit model of muscle trauma, VEGF was supplemented to an area of soft-tissue trauma, and 10 days later, muscle strength and the extent of regeneration were compared to a control group without VEGF supplementation. The group supplemented with VEGF showed improved strength and regeneration compared to the untreated group<sup>49</sup>. Our findings demonstrated an increase in VEGF signal compared to control, suggesting a tendency for the

torn muscle to repair itself for muscle regeneration or to require an increased blood supply to sustain its function.

With our study, it is important to discuss the use of the deltoid as the control muscle for the supraspinatus. The contralateral supraspinatus was not used because 35% of individuals with a rotator cuff tear also have a contralateral tear<sup>6</sup>. Additionally, patients undergoing rotator cuff repair surgery typically only have surgery on one shoulder, so accessibility would also be an issue for a protocol proposed to the Human Ethics Review Board. Similar to the supraspinatus, the ipsilateral deltoid also functions to abduct the arm, exhibits a normal distribution for fiber cross-sectional area<sup>50</sup>, and according to the results of the current study, also demonstrates the same type-I fiber proportion as reported for the supraspinatus in previous studies. Moreover, other studies have also used the deltoid as a control and validated its use, as noted earlier<sup>38,39</sup>.

Nonetheless, there are limitations to this study. The specific location and orientation of fibers biopsied during surgery likely varied, since more than one surgeon collected the different-subject samples. As well, the proportion of fast fibers was deduced from the slow-fiber proportion. Ideally, another set of IHC sections should be stained with antibodies for fast fibers to confirm the present findings on fiber-type distribution, since some fibers can stain positive for more than one myosin isoform. This study is part of a larger study conducted by our research team. Future experiments are examining the innervation status of the torn supraspinatus, which can also change fiber-type and MyHC composition.

## CONCLUSION:

(1) Results from this study demonstrate a shift towards fast fibers and increased angiogenesis signal (VEGF) in pathological supraspinatus muscle after rotator cuff injury ( $p < 0.05$ ). (2) Age, sex, smoking history, time from symptom onset to surgery did not correlate with fiber-type composition or vascularization signal. (3) Similarly, MRI tangent sign, occupancy ratio, and Goutallier score also did not account for differences. (4) Correlation between type I slow fibers and VEGF angiogenesis signal showed a negative slope, but this was not significant ( $p > 0.05$ ).

A shift towards fast fibers and greater VEGF suggests supraspinatus injury, consistent with disuse and/or denervation. Because fiber-type shifts due to disuse atrophy has the potential for muscle to return to its baseline health, knowledge of the muscle innervation status along with the results of this study can provide insight into the overall health of the muscle and allow us to better predict its ability to recover following injury.

## ACKNOWLEDGEMENTS

Thanks to my supervisors Dr Jeff Leiter and Dr Peter MacDonald for all their support and guidance. Special thanks to Dr Judy Anderson for all her support and direction. Also to everyone at Pan Am Clinic Foundation and Deanna Gigliotti for lab technical support. As well, thanks to Dr Greg Stranges, Dr Jason Old, and Dr Jamie Dubberley for their support and involvement with the study.

## REFERENCES

1. Marx, Robert, et al. (2009). Indications for Surgery in Clinical Outcome Studies of Rotator Cuff Repair. *Clinical Orthopaedics And Related Research* 467.2: 450-456.
2. Arce, Guillermo, et al. (2013). Management of Disorders of the Rotator Cuff: Proceedings of the ISAKOS Upper Extremity Committee Consensus Meeting. *Arthroscopy: The Journal of Arthroscopic & Related Surgery* 29.11: 1840-1850.
3. Dunn, W. (2005). Variation in Orthopaedic Surgeons' Perceptions About the Indications for Rotator Cuff Surgery. *The Journal Of Bone And Joint Surgery* 87.9: 1978-1984.

4. Vitale, Mar, et al. (2007). Rotator cuff repair: An analysis of utility scores and cost-effectiveness. *Journal of Shoulder and Elbow Surgery* 16.2: 181-187.
5. Wolf, B, et al. (2007). Indications for Repair of Full-Thickness Rotator Cuff Tears. *The American Journal of Sports Medicine* 35.6: 1007-1016.
6. Yamaguchi, K, et al. (2001). Natural history of asymptomatic rotator cuff tears: A longitudinal analysis of asymptomatic tears detected sonographically. *Journal of Shoulder and Elbow Surgery* 10.3: 199-203.
7. Kim, S, et al. (2013). Fiber type composition of the architecturally distinct regions of human supraspinatus muscle: A cadaveric study. *Histol Histopathol* 28: 1021-1028.
8. Vanhoenacker, F. (2007). *Imaging of Orthopedic Sports Injuries*. Germany: Springer.
9. Walsworth, M, et al. (2004). Diagnosing Suprascapular Neuropathy in Patients With Shoulder Dysfunction: A Report of 5 Cases. *Physical Therapy* 84: 359-372.
10. Codman E. (1984). *The shoulder*. Robert E Kreiger Publishing Co, Philadelphia.
11. Matthews, T. (2006). Pathology of the torn rotator cuff tendon: Reduction in potential for repair as tear size. *Journal of Bone and Joint Surgery - British Volume* 88-B.4: 489-495.
12. Neer, C. S. (1972). Anterior Acromioplasty For The Chronic Impingement Syndrome In The Shoulder. *The Journal Of Bone And Joint Surgery* 87.6: 1399-1399.
13. Bigliani LU et al. (1992). Operative treatment of failed repairs of the rotator cuff. *J Bone Joint Surg Am*. 74:1505–1515.
14. Ozaki, J, et al. (1988). Tears of the Rotator Cuff of the Shoulder Associated with Pathological Changes in the Acromion. *The Journal Of Bone And Joint Surgery* 70-A(8), 1224-1230.
15. Szomor ZL, et al. (2006). Overexpression of nitric oxide synthases in tendon overuse. *J Orthop Res* 24:80–86.
16. Mall, N, et al.. (2014). Current Concepts Review Factors Affecting Rotator Cuff Healing. *The Journal of Bone and Joint Surgery, Incorporated* 96-A(9): 778-88.
17. Gerber, C, et al. (2009). Neer Award 2007: Reversion of structural muscle changes caused by chronic rotator cuff tears using continuous musculotendinous traction. An experimental study in sheep. *Journal of Shoulder and Elbow Surgery* 18.2: 163-171.
18. Rosen ED. (2005). The transcriptional basis of adipocyte development. *Prostaglandins Leukot Essent Fatty Acids* 2005;73:31-4.
19. Cheung, S, et al. (2011). The Presence of Fatty Infiltration in the Infraspinatus: Its Relation With the Condition of the Supraspinatus Tendon. *Arthroscopy: The Journal of Arthroscopic & Related Surgery* 27.4: 463-470.
20. Melis B, et al. (2010). Natural history of fatty infiltration and atrophy of the supraspinatus muscle in rotator cuff tears. *Clin Orthop Relat Res*. 468:1498-505.
21. Senf S, et al. (2008). Hsp70 overexpression inhibits NF-kappaB and Foxo3a transcriptional activities and prevents skeletal muscle atrophy. *FASEB J* 22:3836-45.
22. Rowshan K, et al. (2010). Development of fatty atrophy after neurologic and rotator cuff injuries in an animal model of rotator cuff pathology. *J Bone Joint Surg Am* 92:2270-8.
23. Williamson, D, et al. (2000). Progressive resistance training reduces myosin heavy chain coexpression in single muscle fibers from older men. *J Appl Physiol* 88: 627-633.
24. Malisoux, L, et al. (2006): Effect of long-term muscle paralysis on human single fiber mechanics. *J Appl Physiol* 102: 340-349.
25. Klitgaard, H, et al. (1990). Ageing alters the myosin heavy chain composition of single fibres from human skeletal muscle. *Acta Physiologica Scandinavica* 140(1): 55-62.
26. Pette D, et al. (1997). Mammalian skeletal muscle fiber type transitions. *Int Rev Cytol* 170:143–223
27. Charge, S, et al. (2004). Cellular and molecular regulation of muscle regeneration. *Physiol Rev* 84(1): p. 209-38.
28. Prior B, et al. (2004). What makes vessels grow with exercise training? *J Appl Physiol* 97:1119–1128
29. Makanya A, et al. (2009). Intussusceptive angiogenesis and its role in vascular morphogenesis, patterning, and remodeling. *Angiogenesis* 12(2): 113–123

30. Gianni-Barrera, R et al. (2013). VEGF over-expression in skeletal muscle induces angiogenesis by intussusception rather than sprouting. *Angiogenesis* 16(1), 123-136
31. Vracko R, et al. (1972). Basal lamina: the scaffold for orderly cell replacement. Observations on regeneration of injured skeletal muscle fibers and capillaries. *J Cell Biol* 55:406–419
32. Jarvinen M (1976). Healing of a crush injury in rat striated muscle. A micro-angiographical study of the effect of early mobilization and immobilization on capillary ingrowth. *Acta Patho Microbio Scand* 84:85–94
33. Ferrara N, et al. (1997). The biology of vascular endothelial growth factor. *Endocr Rev* 18:4–25
34. Milkiewicz M, et al. (2003). Differential expression of Flk-1 and Flt-1 in rat skeletal muscle in response to chronic ischaemia: favourable effect of muscle activity. *Clin Sci* 105:473–482
35. Breen E, et al. (1996). Angiogenic growth factor mRNA responses in muscle to a single bout of exercise. *J Appl Physiol* 81, 355–361.
36. Birot, O. J. (2003). Exercise-induced expression of vascular endothelial growth factor mRNA in rat skeletal muscle is dependent on fibre type. *The Journal of Physiology* 552(1), 213-221.
37. Longo, U, et al. (2008). Histopathology of the supraspinatus tendon in rotator cuff tears. *Am J Sports Med* 36(3): 533-8.
38. Ashry, R, et al. (2007). Muscle atrophy as a consequence of rotator cuff tears: should we compare the muscles of the rotator cuff with those of the deltoid? *Skeletal Radiology* 36(9),841-845.
39. Einarsson, F. et al. (2011). Muscle biopsies from the supraspinatus in retracted rotator cuff tears respond normally to passive mechanical testing: a pilot study. *Knee Surgery, Sports Traumatology, Arthroscopy* 19(3), 503-507.
40. Leiter JR, et al. (2012). Nitric oxide and voluntary exercise together promote quadriceps hypertrophy and increase vascular density in female 18-month-old mice. *Am J Physiol Cell Physiol* 302:C1306-15;
41. Upadhyaya, R, et al. (2011). Detecting multiple proteins by Western blotting using same-species primary antibodies, precomplexed serum, and hydrogen peroxide. *Anal Biochem* 419(2), 342-4.
42. Zanetti, M., et al. (1998). Quantitative Assessment of the Muscles of the Rotator Cuff with Magnetic Resonance Imaging. *Investigative radiology* 33(3), 163-170
43. Goutallier, D, et al. (1994). Fatty Muscle Degeneration in Cuff Ruptures. *Clinical Orthopaedics And Related Research* 304, 78-83.
44. Häggmark, T, et al. (1986). Muscle fiber type changes in human skeletal muscle after injuries and immobilization. *Orthopaedics* 9(2), 181-185.
45. Scelsi, R. (2001). Skeletal Muscle Pathology after Spinal Cord Injury: Our 20 Year Experience and Results on Skeletal Muscle Changes in Paraplegics, Related to Functional Rehabilitation. *Basic Appl Myol* 22(2), 75-85.
46. Vijayan K, et al (2001). Fiber-type susceptibility to eccentric contraction-induced damage of hindlimb-unloaded rat AL muscles. *J Appl Physiol* 90: 770 –776.
47. Lexell, J. (1995). Human Aging, Muscle Mass, and Fiber Type Composition. *The Journals of Gerontology* 50A, 11-16.
48. Uhlig, Y. (1995). Fiber Composition and Fiber Transformations in Neck Muscles of Patients with Dysfunction of the Cervical Spine. *Journal of Orthopaedic Research* 13, 240-249.
49. Frey, S, et al. (2012). VEGF Improves Skeletal Muscle Regeneration After Acute Trauma and Reconstruction of the Limb in a Rabbit Model. *Clin Orthop Relat Res* 470, 3607-3614.
50. Macek, B, et al. (2012). Exploring the Biologics of Rotator Cuff Injury And Advancing repair. *B.Sc (Med) Thesis*.

**Table 1:** Summary of Patient Demographics.

	N	Mean	SD	Min	Max
<b>Age</b>	27	56.9	5.4	45	66
<b>Sex</b>	27	20 Male; 7 Female			
<b>BMI</b>	27	28.8	4.3	21.1	38.4
<b>Smoking</b>	27	19 No; 8 Yes			
<b>Time from Symptom Onset to MRI (weeks)</b>	25	41.9	92.1	2	476
<b>Time from Symptom Onset to Surgery (weeks)</b>	26	72.9	94.5	12	520

**Table 2:** Summary of Patient MRI data.

	N	Mean	SD	Min	Max
<b>MRI – Tear Size (cm)</b>	25	1.9	0.9	0.8	4.6
<b>MRI – Tear Thickness</b>	26	24 Full-Thickness; 2 Partial-Thickness			
<b>MRI – Tendons Involved</b>	58	26 Supraspinatus; 5 Infraspinatus; 2 Teres Minor			
<b>MRI – Tangent Sign</b>	21	18 Negative; 3 Positive			
<b>MRI – Occupancy Ratio</b>	21	0.8	0.2	0.3	1.2
<b>MRI – Goutallier Sign</b>	21	0.9	0.8	0	3

**Table 3:** Patient Demographic and MRI data for each study participant.

Patient ID	Age	Sex	Smoking Hx	Onset of Symptoms to Surgery (weeks)	MRI: Tear Thickness	MRI: Tangent Sign	MRI: Occupancy Ratio	MRI: Goutallier score
01	65	F	Y	73	PT	Negative	0.85	1
02	49	M	N	33	FT	Negative	0.85	1
03	57	M	N	23	FT	Negative	0.71	1
04	59	M	N	56	FT	Negative	0.83	1
06	62	M	N	57.5	FT	Negative	0.86	2
07	62	M	Y	520	FT	Positive	0.31	3
08	56	M	Y	69	FT	–	–	–
09	65	M	N	61.5	FT	Negative	0.61	0
10	58	F	N	38	FT	Negative	0.80	1
11	52	F	N	17.5	FT	Negative	0.96	1
12	49	M	N	56	FT	Negative	0.89	1
13	56	F	Y	51	–	–	–	–
14	59	M	N	72	FT	Negative	0.55	1
16	62	M	N	58	FT	Negative	0.88	0
17	53	F	Y	81	FT	Negative	0.89	1
18	56	M	N	40	PT	Negative	1.15	1
19	58	M	N	-	FT	Negative	0.93	0
20	53	F	Y	43	FT	Negative	0.84	1
22	60	M	N	24	FT	Positive	0.57	2
23	52	M	N	114	FT	Negative	0.97	0
24	49	M	N	39	FT	Negative	0.80	0
26	60	F	N	64	FT	Negative	0.91	1
27	55	M	Y	12	FT	Positive	0.52	1
28	45	M	N	59	FT	–	–	–
29	66	M	N	73	FT	–	–	–
31	61	M	N	47	FT	–	–	–
32	57	M	Y	113	FT	Negative	0.81	0

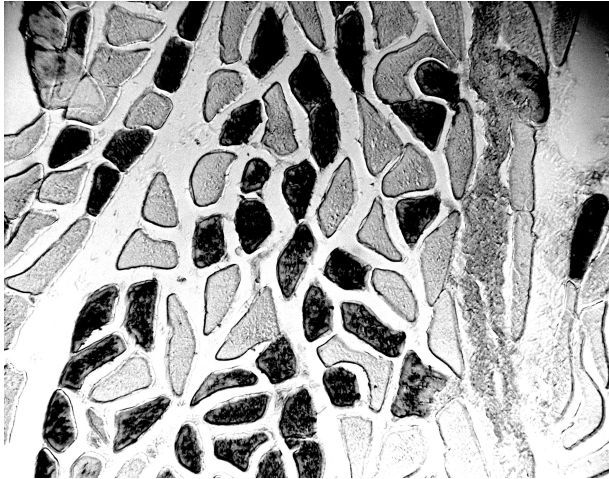


**Figure 1a:** Immunostaining for type I muscle fibers in transverse section.

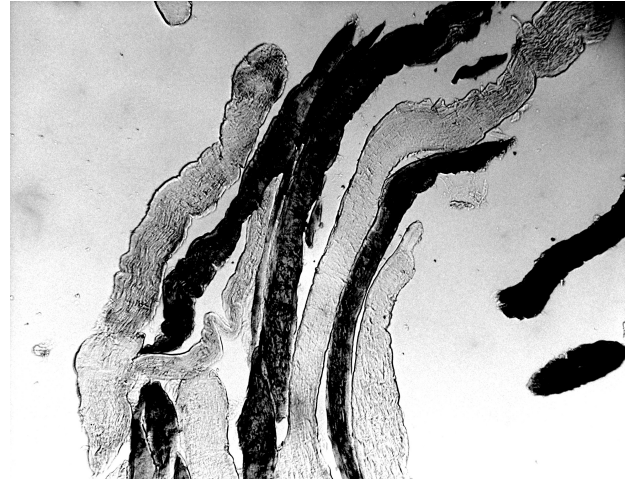


**Figure 1b:** Immunostaining for type I muscle fibers in longitudinal section.

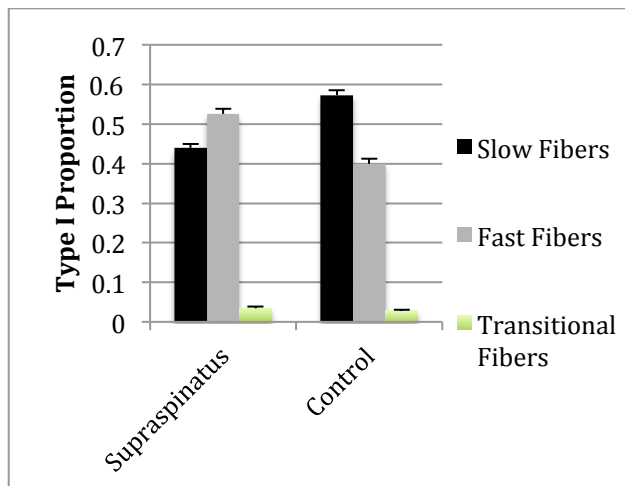


**Figure 2:** Muscle fiber type composition in pathological supraspinatus muscle versus control muscle (from immunostaining). The entire biopsy sample was imaged, and 31259 fibers were counted in total.

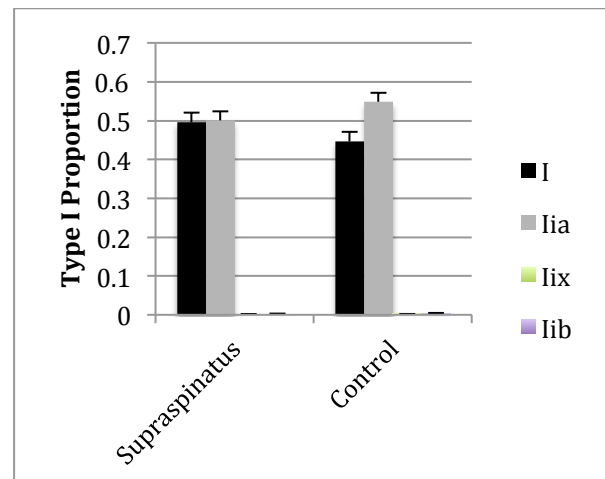


**Figure 3:** MyHC isoform composition in supraspinatus versus control by Western blot.

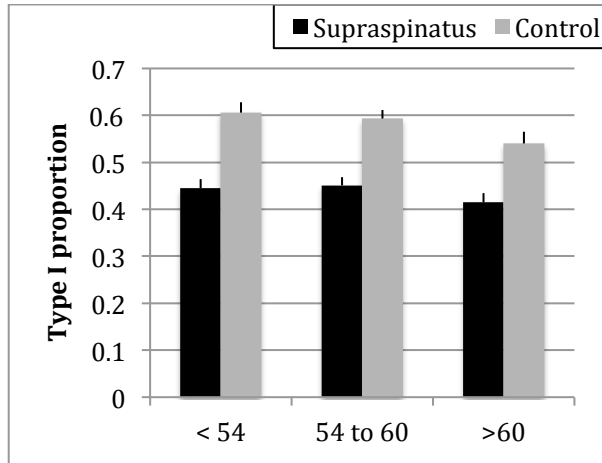


**Figure 4a:** Type I fiber proportions broken down by Age.

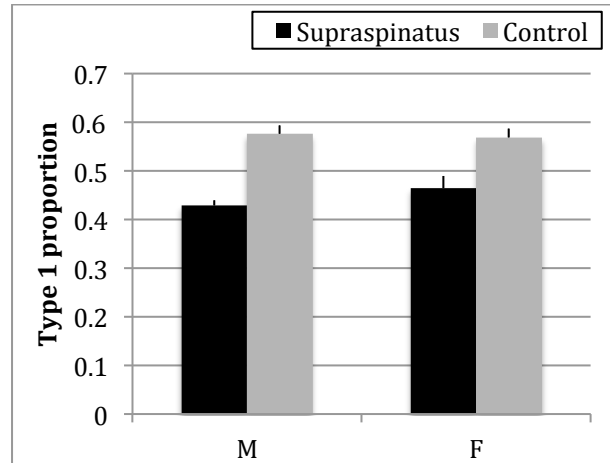


**Figure 4b:** Type I fiber proportions broken down by Sex.

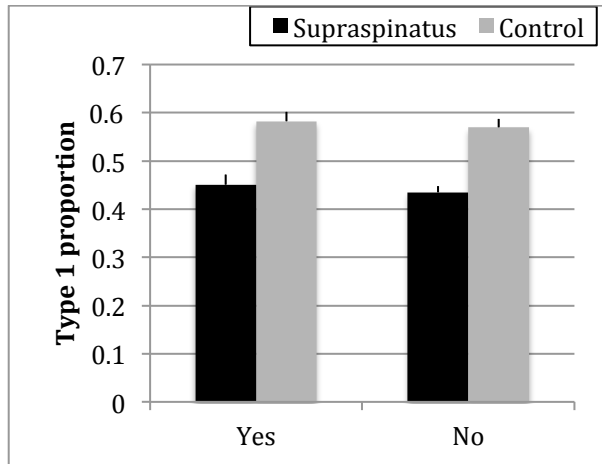


**Figure 4c:** Type I fiber proportions broken down by Smoking History.

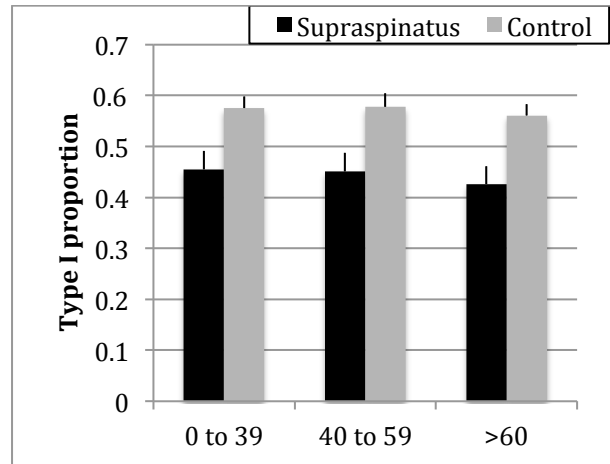


**Figure 4d:** Type I fiber proportions broken down by Time from Symptom onset to surgery.

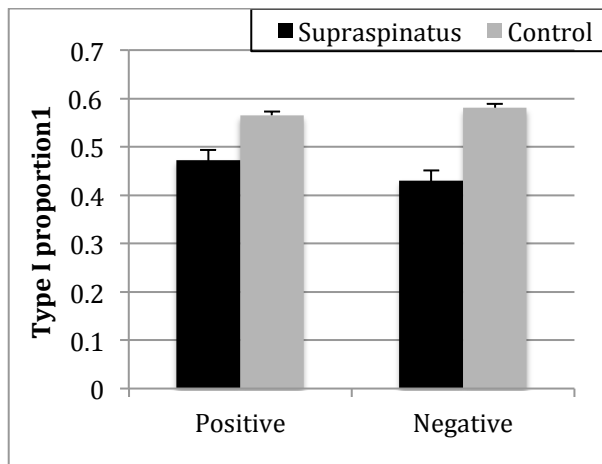


**Figure 5a:** Type I fiber proportions broken down by MRI Tangent sign.

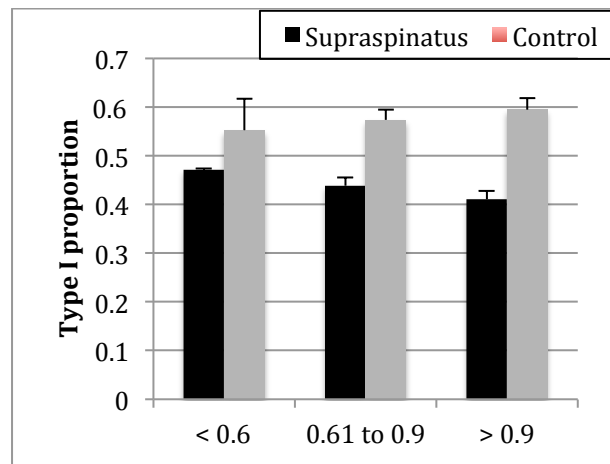


**Figure 5b:** Type I fiber proportions broken down by MRI Occupancy Ratio.

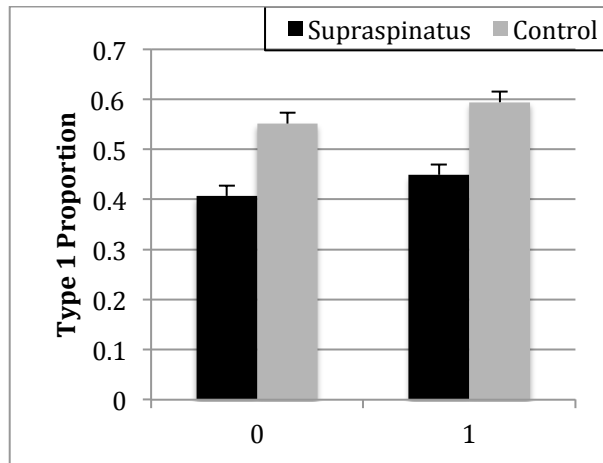


**Figure 5c:** Type I fiber proportions broken down by MRI Goutallier score.

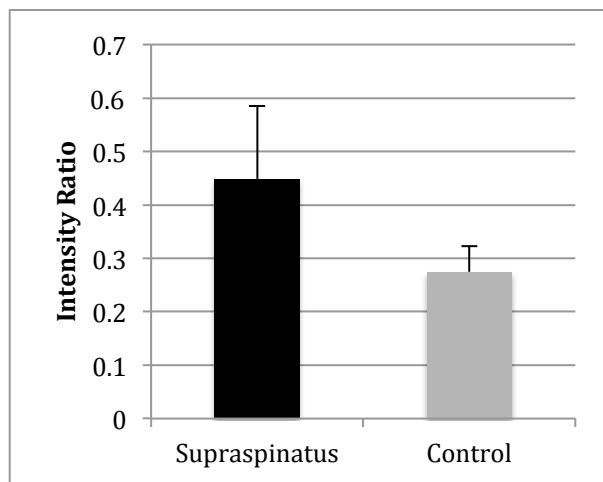


**Figure 6a:** VEGF WB comparing supraspinatus versus control (VEGF normalized to beta-actin).

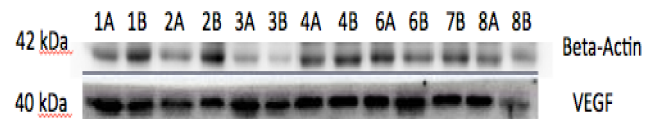


**Figure 6b:** VEGF WB from study participants (A=supraspinatus; B=control) with beta-actin control.

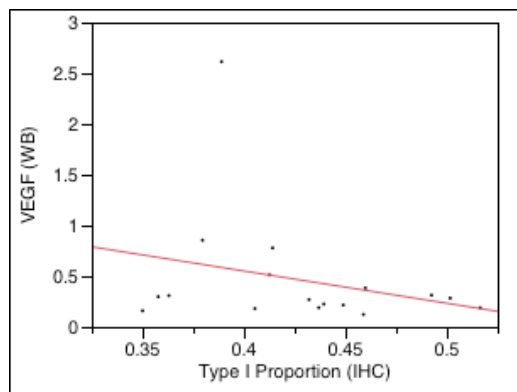


**Figure 7:** Correlation between VEGF (WB) and Type I Proportion (IHC). Line of best fit shows a negative slope but  $p > 0.05$ .